Contents list available at CBIORE journal website

International Journal of Renewable Energy Development

Journal homepage: https://ijred.cbiore.id

Research Article

Comparison of lithium sources on the electrochemical performance of $LiNi_{0.5}Mn_{1.5}O_4$ cathode materials for lithium-ion batteries

Sudaryanto[a*], Nadhifah Salsabila[b], Puspita Ayu Kusuma Sari[b], Adinandra Caesar Fachrudin[c], Adinda Atalya Salsabila[b], Eduardus Budi Nursanto[b], Slamet Priyono[a], Heri Jodi[a], Muhammad Dikdik Gumelar[d]

[a]*Research Center for Advanced Materials, National Research and Innovation Agency, Banten 15314, Indonesia*

[b]*Department of Chemical Engineering, Universitas Pertamina, Jakarta 12220, Indonesia*

[c]*Department of Chemical Engineering, Universitas Gadjah Mada, Yogyakarta 55281, Indonesia*

[d]*Research Center for Conversion and Conservation Energy, National Research and Innovation Agency, Banten 15314, Indonesia*

Abstract. In order to fulfill the demand for high energy and capacity, an electrode with high-voltage capability, namely $LiNi_{0.5}Mn_{1.5}O_4$ (LNMO) that has an operating potential of up to 4.7 V vs Li/Li^+, is currently becoming popular in Li-ion battery chemistries. This research produced LNMO by using a solid-state method with only one-step synthesis route to compare its electrochemical performance with different lithium sources, including hydroxide (LNMO-LiOH), acetate (LNMO-LiAce), and carbonate (LNMO-LiCar) precursors. TGA/DSC was first performed for all three sample precursors to ensure the optimal calcination temperature, while XRD and SEM characterized the physical properties. The electrochemical measurements, including cyclic voltammetry and charge-discharge, were conducted in the half-cell configurations of LNMO//Li-metal using a standard 1 M $LiPF_6$ electrolyte. LNMO-LiOH samples exhibited the highest purity and the smallest particle size, with values of 93.3% and 418 nm, respectively. In contrast, samples with higher impurities, such as LNMO-LiCar, mainly in the form of $Li_xNi_{1-x}O$ (LiNiO), displayed the largest particle size. The highest working voltage possessed by LNMO-LiOH samples was 4.735 V vs Li/Li^+. The results showed that LNMO samples with LiNiO impurities would affect the reaction behavior that occurs at the cathode-electrolyte interface during the release of lithium-ions, resulting in high resistance at the battery operations and decreasing the specific capacity of the LNMO during discharging. The highest value, shown by LNMO-LiOH, was up to 92.75 mAh/g. On the other side, LNMO-LiCar only possessed a specific capacity of 44.57 mAh/g, indicating a significant impact of different lithium sources in the overall performances of LNMO cathode.

Keywords: Li-ion Battery, Cathode, LNMO, Precursor, Solid-State

Received: 14th Nov 2023; Revised: 18th February 2024; Accepted: 23rd March 2024; Available online: 2nd April 2024

1. Introduction

Lithium-ion batteries (LIBs) are favored for various applications, including portable electronics, intermittent renewable energy storage, electric vehicles, and power grids, due to their high energy density and long lifespan (Mohamed & Allam, 2020; Mossali *et al.*, 2020). However, further strategies are still needed to enhance the energy storage capacity of LIBs to meet the diverse demands of various applications (Choi *et al.*, 2020; Tian *et al.*, 2021). Achieving LIBs with high energy capability can be accomplished by either raising the cathode's operating potential or enhancing the cathode's and anode's capacity (Chen *et al.*, 2021; J. Li *et al.*, 2017).

The cathode material has a reasonably significant role in LIB, as it must have fast storage and release of lithium-ions during battery charging. At present, commonly used cathode materials in LIBs include $LiCoO_2$ (LCO), $LiFePO_4$ (LFP), $LiMn_2O_4$ (LMO), as well as Ni-containing like $LiNi_xMn_yCo_{1-x-y}O_2$ (NMC) and $LiNi_xCo_yAl_{1-x-y}O_2$ (NCA) (Ahsan *et al.*, 2021; Y. Li *et al.*, 2021). Of all elements, cobalt has major challenges due to its relatively high cost, concerns about environmental impacts and human rights issues in its mining activity. Recently, Co-free $LiNi_{0.5}Mn_{1.5}O_4$ (LNMO) cathode materials have received considerable interest due to their distinct advantages, notably its high operating potential plateau at 4.7 V vs Li/Li^+, acceptable cycle lifespan, and excellent stability in thermal resistance (Chi *et al.*, 2010; Ghosh *et al.*, 2021; Ma *et al.*, 2018). Due to its high-voltage capability, LNMO has the advantage of offering approximately 20% higher energy density compared to traditional LCO and about 30% higher energy density compared to commercial LFP, making it an attractive choice for advanced LIB applications (Yi *et al.*, 2016). Furthermore, the increase in energy density by incorporating nickel makes it the lowest cell material cost per kWh compared to other Mn-based cathode materials (Murdock *et al.*, 2021).

* Corresponding author
Email: suda014@brin.go.id (Sudaryanto)

https://doi.org/10.61435/ijred.2024.59662
ISSN: 2252-4940/© 2024.The Author(s). Published by CBIORE

However, LNMO has many challenges, particularly for applications with high-power requirements, such as low cycle performance when applying high current rates (Fakhrudin *et al.*, 2021; Sudaryanto *et al.*, 2021). The primary issue with LNMO is the occurrence of degradation reactions in high-voltage operation that potentially cause corrosion reactions in the interface region between the cathode and electrolyte, resulting in low rate stability, especially at high temperatures (Ghosh *et al.*, 2021; Yi *et al.*, 2016). Therefore, several previous studies have majorly explored many aspects of modification, such as coating (Ku *et al.*, 2019), structure (Yi *et al.*, 2009), morphology (Lin *et al.*, 2023), electrolyte optimization (Guo *et al.*, 2022), and element doping (Kosova *et al.*, 2016).

LNMO can be synthesized through various methods, including sol-gel (Xu *et al.*, 2017), sonochemistry (Sivakumar *et al.*, 2015), solid-state (W. Wu *et al.*, 2023), co-precipitation (Shen *et al.*, 2020), and hydrothermal synthesis (Yi *et al.*, 2017). The solid-state method seems to be the most established method for obtaining well-crystallized LNMO particles at low cost (W. Wu *et al.*, 2023). Other results with some improvements at high heating and cooling rates in the air exhibit a specific capacity, achieving close to its theoretical value, up to 143 mAh/g (Luo *et al.*, 2023; Whittingham, 2004). These findings indicate that these methods are preferable for LNMO synthesis to enhance its performance, which can be prepared in two distinct ways, first by directly combining all precursors in one-step reaction and other with the two-step process by involving the initial anion preparation followed by the subsequent incorporation of lithium (Feng *et al.*, 2011; W. Wu *et al.*, 2023).

On the other side, lithium sources or precursors as a critical element for the cathode materials can be found in various forms, mainly lithium hydroxide (LiOH) or lithium carbonate (Li_2CO_3), as both hold the most production from ore or brine-based resources worldwide. Despite LiOH having more fluctuating purity and corrosivity than Li_2CO_3, it provides higher discharge capacity and retention and lower sintering temperature for obtaining stable structure (Murdock *et al.*, 2021). However, LiOH generally needs a further conversion process from Li_2CO_3, so in other considerations, brine resources are cheaper to refine as they require one less step (Nguyen *et al.*, 2023). Other metal components are typically sourced as nitrate or sulfate-based and potentially release pollutant gas like nitrogen oxide (NO_x) and sulfur oxide (SO_x) into the atmosphere and eventually generate acid rain (Kelly *et al.*, 2020; Marceau *et al.*, 2010). Therefore, precursors from acetate-based become an alternative option for reducing greenhouse gas emissions and environmental impacts and for the sustainability of LIB productions.

Besides the synthesis route, previous research has shown remarkable achievement in comparing different lithium sources for serving diverse electrochemical performances (Ma *et al.*, 2018). For example, Li-rich cathode materials prepared by co-precipitation exhibit better electrochemical performances with Li_2CO_3 precursors (Y. Wang *et al.*, 2023; C. Wu *et al.*, 2022), while other cathode structures with different synthesis methods, including LMO via solid-state (P.-B. Wang *et al.*, 2018), LFP via sol-gel (Hu *et al.*, 2013), and NMC via spray pyrolysis (Ihalainen *et al.*, 2023), showed prominent result with LiOH. The type of lithium sources can determine the structural transformation during the heating treatment, which controls the morphology and surface of the resulting materials and, as a result, provides different electrochemical performances. Moreover, other researchers studied in more detail lithium source variations like acetate, nitrate, phosphate, or fluoride (Cao *et al.*, 2017; Zhang *et al.*, 2014; Zybert *et al.*, 2020). Hence, the appropriate choice will need further optimization regarding the obtained cathode materials and synthesis routes for achieving synergistic properties and performance in battery applications.

Selecting the right lithium precursor is crucial for effectively integrating lithium ions into the nickel manganese oxide structure for preparing the spinel LNMO. However, to the best of our knowledge, no systematic study has been done so far, specifically for high-voltage LNMO cathodes. Previous studies comparing more than two types of precursors have only shown that different lithium sources contributed to various properties and performances of cathode materials with diverse synthesis routes (Cao *et al.*, 2017; Hu *et al.*, 2013; Ihalainen *et al.*, 2023; P.-B. Wang *et al.*, 2018; Zhang *et al.*, 2014; Zybert *et al.*, 2020). This study aims to synthesize LNMO cathode materials using various lithium sources, including hydroxide, acetate, and carbonate, with a one-step solid-state reaction mechanism to investigate the differences in morphology, structure, impurity, and properties, as well as elucidate the significant effect in the electrochemical performances, including discharge capacity and its stability operated in a high number of cycling.

2. Materials and Methods

2.1. Materials Synthesis

The active material of LNMO was prepared via a one-step solid-state synthesis route with different lithium sources, including lithium hydroxide (LiOH, >98%), lithium acetate ($LiCH_3COO$, 99.95%), and lithium carbonate (Li_2CO_3, 99.99%), purchased from Sigma Aldrich. The other precursor for preparing the spinel LNMO structure used acetate-based nickel and mangan, including nickel acetate ($Ni(CH_3COO)_2{\cdot}4H_2O$, >98%) and manganese acetate ($Mn(CH_3COO)_2{\cdot}4H_2O$, >99%), obtained from Thermo-Scientific. All chemicals were used as received without any further purification. Then, all materials were put together in a stoichiometric ratio of lithium, nickel, and mangan precursors and milled using a planetary ball mill with a ratio of materials to a ball of 1:5 at a speed of 200 rpm for about 2 hours. After being mixed evenly, the mixture, in the form of powder, is dried at 50 °C for 12 hours in an oven vacuum and continued by ground and pelletized. Three different pellets were prepared using various lithium sources and were marked as LNMO-LiOH (hydroxide), LNMO-LiAce (acetate), and LNMO-LiCar (carbonate). Different from the previously reported study (P.-B. Wang *et al.*, 2018), pellets were priorly calcinated at 400 °C for 5 hours before being sintered at a high-temperature environment of up to 800 °C (heating rate 3 °C/min) for about 24 hours in a muffle furnace. Finally, the resulting samples of LNMO active materials were ground and sieved to obtain a homogeneous fine powder under 400 mesh size.

2.2. Characterization Techniques

Thermal behavior was analyzed by thermogravimetric analysis and differential scanning calorimetry (TGA/DSC) of the dried mixture of precursors before high-heating treatment to obtain the optimal temperature for the calcination process using a SETARAM TG/DSC instrument within a temperature range between room temperature of about 30 to final temperature of 800 °C (heating rate 10 °C/min) under airflow atmosphere. Crystal structures of the produced LNMO cathode materials were analyzed by X-ray diffraction (XRD) using Malvern PANanalytical instrument with Cu Kα radiation (λ= 1.5418 Å) within Bragg angles (2θ) between 5° and 80° (scan rate 3°/min)

at room temperatures (Sudaryanto *et al.*, 2021). Analyzation of the obtained XRD pattern was examined using X'Pert Highscore software. Surface morphology was collected by scanning electron microscopy and energy-dispersive X-ray spectroscopy (SEM-EDS) for the synthesized LNMO cathode materials using a JEOL JSM-6510LA, and the resulting image was examined using Image-J software on the material's morphology to evaluate its particle size and distribution.

2.3. Electrochemical Performances

Electrochemical performances were measured by preparing CR2032-type coin cells. Active materials of LNMO in a mass ratio of 80% were put together with 10% conductive super P carbon black (CB, MTI) and 10% polyvinylidene fluoride (PVDF) in N, N-dimethylacetamide (DMAc, Merck) solvent to prepare the slurry mixture for the cathode. Next, the slurry mixture, which had achieved homogenous conditions, was poured into the aluminum sheet surface as a current collector, coated using a doctor blade method, and continued by drying at a temperature of 80 °C for 1 day in the vacuum oven. After that, the cathode sheet was die-cut and assembled by incorporating lithium metal as the anode, polypropylene (PP, Celgard) sheet as a separator, and 1 M lithium hexafluorophosphate ($LiPF_6$) electrolyte in carbonate-based solvents of EC/DEC/DMC with a ratio of 1:1:1 (w/w), operated in a glove box filled with inert argon gas (O_2 < 1 ppm, H_2O < 1 ppm). The assembled coin cell was first cleaned with ethanol prior to the electrochemical measurements. Redox reaction behavior was examined by cyclic voltammetry (CV), while battery test performance was analyzed by charge-discharge (CD), both evaluated at room temperatures. CV was cycled in a potential window between 3.5 and 5.5 V (scan rate 0.1 mV/s) using Automatic Battery Cycler WBCS3000 (WonATech), while CD was tested in a constant current and constant voltage (CC-CV) mode with a cut of voltage between 3.50 and 4.95 V (current rate C/10) using Battery Analyzer BST8-WA (MTI Corporation).

3. Results and Discussion

TGA/DSC was conducted on the mixed precursor containing lithium, nickel, and mangan under an airflow atmosphere to obtain the optimal calcination temperature and investigate the significance of various lithium precursors. As shown by TGA/DSC curves in Figure 1, all samples indicate mass loss in two different primary stages, appearing in the temperature range of 100 °C to approximately 200 °C and 200 - 500 °C, respectively. Further high heating up to 800 °C remained

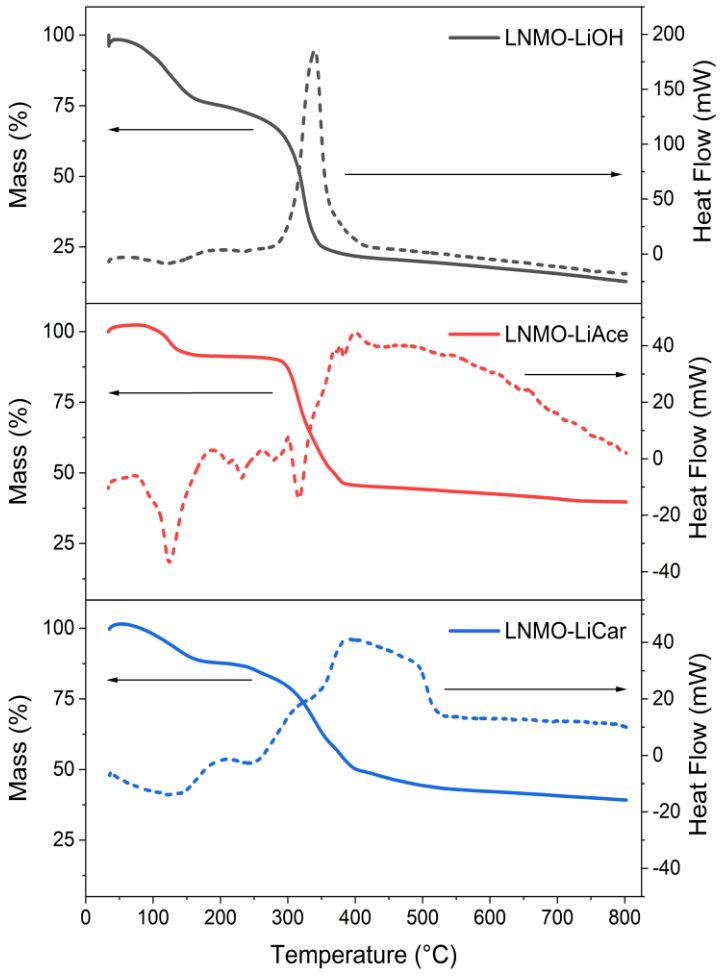

Fig 1. Sample mass and heat flow as a function of heating temperature obtained from TGA/DSC measurements in different lithium sources.

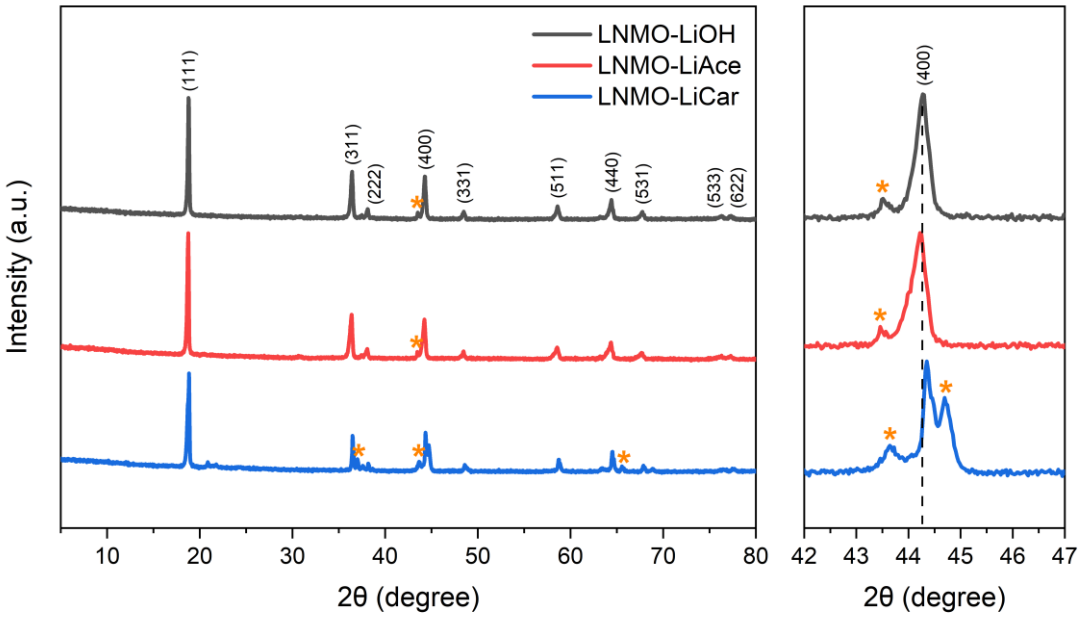

Figure 2. XRD patterns of different lithium sources for the synthesized LNMO cathode materials.

Table 1
Lattice parameters of different lithium sources for the synthesized LNMO cathode materials.

Sample	LNMO-LiOH	LNMO-LiAce	LNMO-LiCar
a (Å)	8.1838	8.1829	8.1522
V (Å^3)	548.1253	547.9381	541.7899
$I_{(311)}/ I_{(400)}$	1.0158	1.0301	0.9341
Purity (%)	93.3	85.1	69.4

unchanged, with no significant mass loss appearing on the mixed precursors. The first stage consists of a gradual mass loss corresponding with endothermic reactions due to the release of non-oxidative decomposition from hydration water owned by nickel acetate and manganese acetate (Ronduda *et al.*, 2020; Ulu Okudur *et al.*, 2022). These results indicate that the drying process at 50 °C for 12 hours was insufficient to completely remove hydrate from the precursors. In contrast, the second stage has a major mass loss of about 40%, which may be related to the oxidative decomposition of all precursors and the exothermic reactions between lithium sources with nickel acetate and manganese acetate (Liu *et al.*, 2018; T. Wu *et al.*, 2015). Although LNMO-LiOH has a lower stable region with a lower temperature peak in the second stages, the basis for selecting the optimal calcination temperature from TGA/DSC results was at 400 °C, continued by subsequently heated to 800 °C for the sintering process to enhance the crystallinity and form stable structures.

The diffraction patterns of the synthesized LNMO using different lithium sources are given in Figure 2. All samples generally exhibit intense and narrow peaks, suggesting a high degree of crystallinity, and are consistent with the Rietveld refinement profiles of LNMO in the ICSD 98-18-2847 database using X'Pert Highscore software, indicating a successful synthesis of the spinel LNMO. Peaks labeled with *hkl* indexes referred to the LNMO cathode materials in the spinel phase, and the impurity phase of each obtained sample was represented by peaks marked with (*), in which peak intensity can be due to the difference in morphology and particle size (Ulu Okudur *et al.*, 2022). Since there are impurities found in all samples in the form of $Li_xNi_{1-x}O$ (LiNiO), the obtained LNMO cathode materials have two different space groups, showing Fd-3m disordered structure rather than $P4_332$ ordered one, consisting of a single-phase of FCC structure. LNMO-LiCar has more LiNiO phase than the other two lithium sources, related to the decomposition process of urea as a result of carbonate-based lithium sources from anion released (Qin *et al.*, 2019). The presence of impurities related to the synthesis route using a one-step solid-state method results in the non-uniformity of mixed precursors and oxygen loss at high temperatures, agreeing with the previously reported studies (Feng *et al.*, 2011; W. Wu *et al.*, 2023). It should be noted that the heating treatment used in this study was carried out in a muffle furnace without additional airflow, causing a lack of oxygen during the calcination and sintering process.

Lattice parameters of the synthesized LNMO calculated from the diffraction peaks are shown in Table 1. As previously mentioned, all samples belong to the Fd-3m ordered space group, representing a cubic-based structure, so it has exactly the same lattice parameters: $a = b = c$. Li atoms take the 8a tetrahedral sites in this space group, while Ni and Mn atoms randomly reside in the 16d octahedral sites (Sivakumar *et al.*,

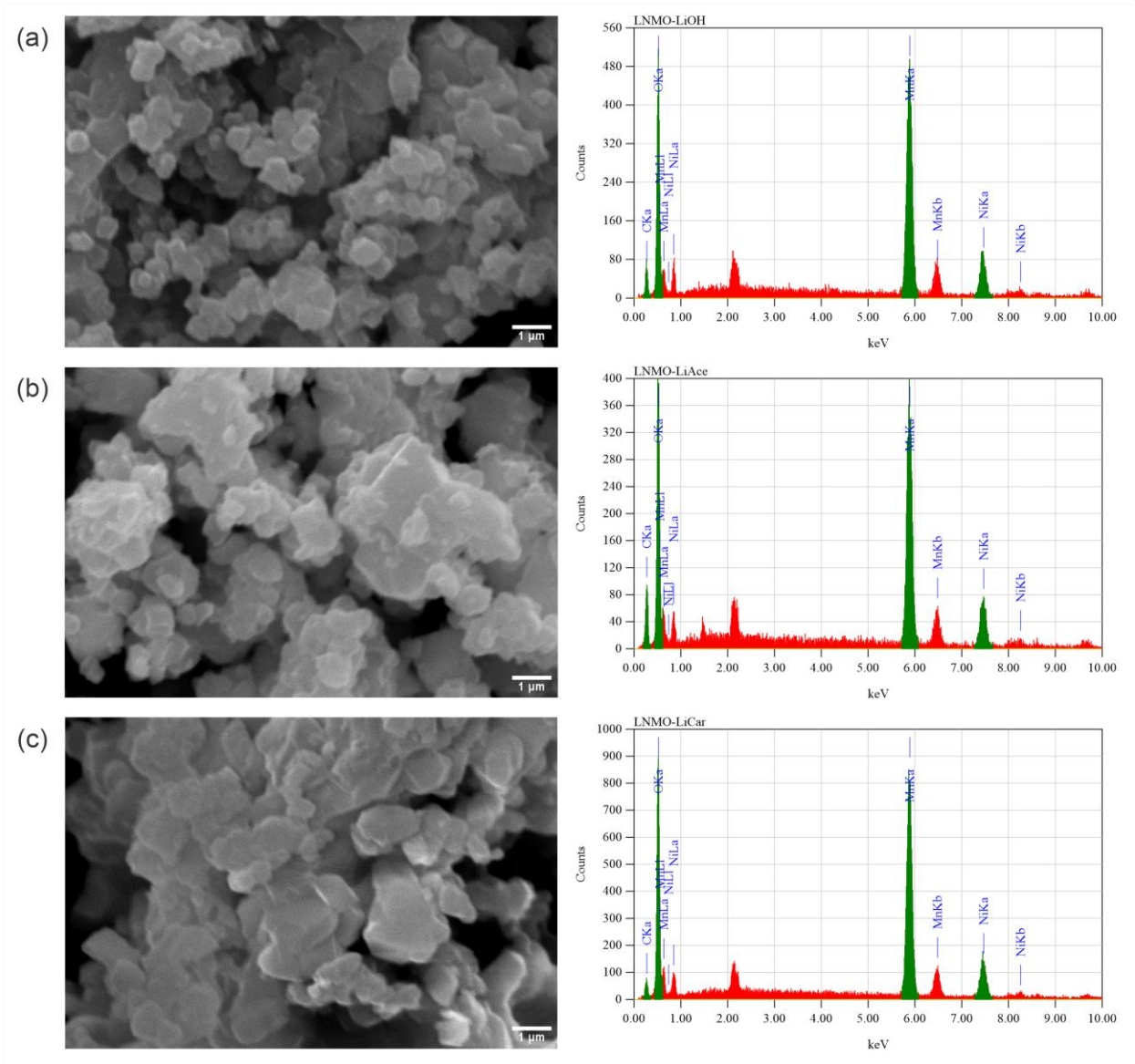

Fig 3. SEM images equipped with EDS spectra of LNMO cathode materials synthesized from lithium (a) hydroxide, (b) acetate, and (c) carbonate precursors.

Table 2
Elemental compositions from EDS spectra of LNMO cathode materials synthesized from different lithium sources.

Sample	LNMO-LiOH	LNMO-LiAce	LNMO-LiCar
Ni (%)	8.31	7.36	8.01
Mn (%)	26.64	23.21	27.29
O (%)	65.05	69.43	64.70

2015). LNMO-LiCar has the smallest lattice parameters and intensity ratios, while LNMO-LiOH and LNMO-LiAce have comparable values of around 8.18 Å and 1.0, respectively. The increased lattice parameters and the decreased intensity ratios indicate lower distortion phenomena with a great improvement in structural stability due to stronger bonding between Ni and Mn atoms with O atoms (Luo *et al.*, 2023). From Rietveld refinement profiles, impurity from the contribution of LiNiO can also be calculated. LNMO-LiCar has the smallest spinel phase of only 69.4%, showing a similar trend due to low lattice parameters with a high impurity phase. These impurities can potentially block the major structure of the LNMO cathode materials by decreasing Ni content and Mn valence, reducing

the active sites for Li ions transfer, and causing poor electrochemical performances (Yi *et al.*, 2009).

The sample morphologies of the obtained LNMO observed through SEM-EDS measurements are depicted in Figure 3. All samples showed rough surface morphology and agglomerated particles with different particle sizes and distribution. Significant differences can be observed in the SEM images as the effect of different lithium sources even though it has been through post-synthesis treatment like grinding and sieving for achieving particle homogeneity. Image-J software processing shows that the average lengths of particles for lithium hydroxide, acetate, and carbonate precursors are 418, 514, and 562 nm, respectively. Notably, LNMO-LiOH exhibits the smallest particle size and distribution, confirming the XRD results with higher structural stability. The large particle size observed in LNMO-LiCar is assumed to be the effect of high impurity content in the sample. Size difference and distribution can be attributed to the synthesis process, including the mixing of precursors and the effect of high heating temperatures up to 800°C (Zeng *et al.*, 2021). It's worth noting that smaller particle sizes result in larger surface areas, facilitating easier ionic transfer.

SEM measurement has been equipped with EDS for identifying elemental compositions of the obtained materials, as listed in Table 2. Ideally, LNMO cathode materials have an elemental ratio of Ni, Mn, and O atoms 1:3:8. Therefore, the EDS spectra have been conducted only in those atoms, excluding Li. The obtained LNMO mostly demonstrated similar atomic stochiometrics with an elemental ratio of Ni, Mn, and O atoms of about 1:3:8, confirming the formation of the LNMO structure.

The electrochemical behavior of the three different lithium precursors of the synthesized LNMO sample is shown as cyclic voltammogram profiles in Figure 4. The curves provide a similar tendency in which all samples have two types of peaks, containing two of each oxidation and reduction peak. The oxidation peak at around 4.0 V corresponds to the occurrence of the oxidation reaction of Mn^{3+} to Mn^{4+}, and that at around 5.0 V corresponds to the oxidation of Ni^{2+}/Ni^{3+} to Ni^{4+} (Kong *et al.*, 2023; Palaniyandy *et al.*, 2022). The oxidation/reduction at high voltage of LNMO-LiOH, LNMO-LiAce, and LNMO-LiCar occur at 5.00/4.47 V, 4.96/4.43 V, and 4.86/4.53 V, resulting in a voltage difference of 0.53 for the first two samples and 0.33 V for LNMO-LiCar. The redox peaks of LNMO-LiCar have a

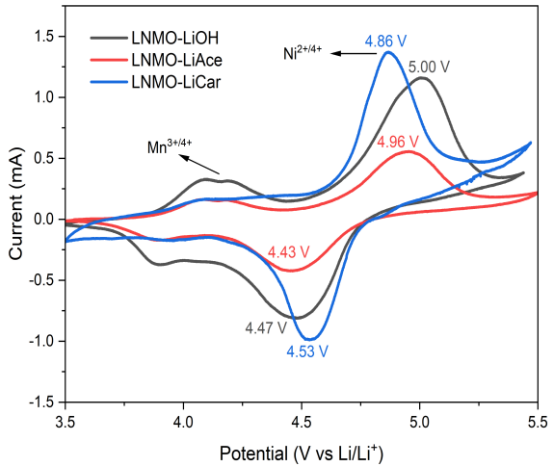

Fig 4. CV curves of LNMO prepared by different lithium sources (hydroxide, acetate, carbonate) at 0.1 mV/s scan rates from 3.5 to 5.5 V of the potential window.

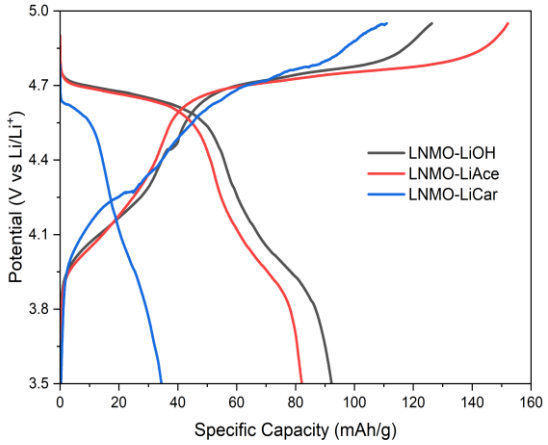

Fig 5. CD curves in the 4th cycle of LNMO prepared by different lithium sources (hydroxide, acetate, carbonate) at C/10 current rates from 3.50 to 4.95 V of cut of voltage.

voltammogram profile, which is relatively symmetric compared with the other two, thus providing the electrochemical reaction with better reversibility. Among all samples, LNMO-LiCar also exhibits the smallest potential difference between the redox peaks, meaning that this sample provides the best electrochemical reversibility performance and reaction kinetics (Ma *et al.*, 2018). Although in terms of reversibility, showing better results in LNMO-LiCar, LNMO-LiOH samples have advantages in a slightly higher operating potential of 4.735 V vs Li/Li^+.

The electrochemical capacity of the LNMO sample, prepared using three different lithium precursors, is shown as charge-discharge profiles in Figure 5. The curves were taken at room temperatures with initial C/10 current rates and showed in the 4th cycle, which is assumed to be a relatively stable cycle after the formation step. From the charge-discharge profile, all samples display two potential plateaus at around 4.0 V and 4.8 V, which corresponds to the redox reaction of Mn^{3+}/Mn^{4+} and Ni^{2+}/Ni^{4+}, respectively, and in accordance with the previous CV measurement (Mohamedi *et al.*, 2002). However, all samples show different values of specific capacity during both charging and discharging. Discharge capacity for LNMO-LiOH, LNMO-LiAce, and LNMO-LiCar samples are 92.75, 73.46, and 44.57 mAh/g, respectively. LNMO-LiOH exhibits the highest discharge capacity, followed by LNMO-LiAce and then LNMO-LiCar. These results are in accordance with SEM analysis that shows the smaller particle size, the greater the capacity, but in contrast with the CV measurement in which LNMO-LiCar depicted the best electrochemical reversibility and reaction. The most common impurity found in LNMO is LiNiO, mainly due to incomplete reactions in the synthesis process, which is assumed to be the main contributor to the poor discharge capacity in the case of LNMO-LiCar. The formation of LiNiO causes a reaction with the electrolyte and the release of Li^+ and large resistance during the charging and discharging period so that the capacity of LNMO can decrease (Zeng *et al.*, 2021).

The electrochemical retention of each sample has been evaluated for 100 cycles at C/5 current rates in a voltage range from 3.50 to 4.95 V, as shown in Figure 6. Although LNMO-LiOH and LNMO-LiAce exhibit better discharge capacity, they have poor cycle stability, showing similar retention around the 40th cycle, compared to LNMO-LiCar. SEM images have

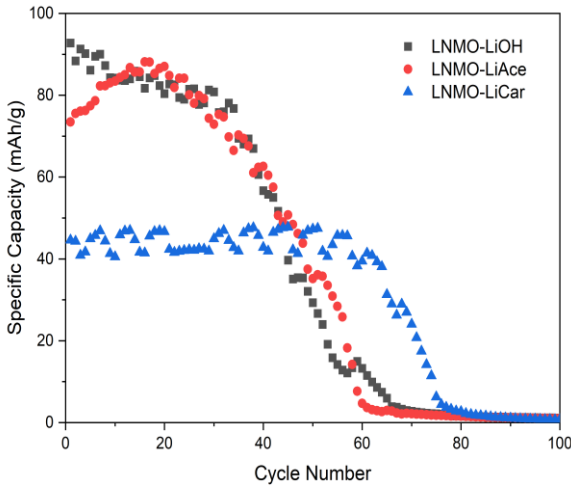

Fig 6. Cycling performance of different lithium sources for the synthesized LNMO cathode materials.

revealed that LNMO-LiCar has a large particle size, causing a long distance in the lithium-ion transfer path, resulting in a smaller capacity, increasing unnecessary impurities, and reducing the material purity of the obtained LNMO sample (Zeng *et al.*, 2021). After certain cycles, side reactions will occur on the surface between the electrode and electrolyte, forming solid electrolyte interphase (SEI) and decreasing the specific capacity (Lang *et al.*, 2022). Therefore, small particle size can effectively reduce the occurrence of side reactions at the electrode-electrolyte interface. However, the degradation of metal content on the electrolyte can also influence capacity retention. Despite their high cycle stability, the LiNiO impurities in LNMO-LiCar are assumed to contribute as a blocking layer for metal degradation of LNMO, making it unreliable for comparison with the other two samples. These impurities, in other words, can positively protect the LNMO structures but, as a result, inhibit the high electrochemical performances of the LNMO cathode materials.

4. Conclusion

In summary, LNMO has been successfully synthesized using a one-step solid-state method from acetate-based precursors mixed with different lithium sources, including hydroxide, acetate, and carbonate. All variations were calcinated at 400 °C before the sintering process at 800 °C based on the optimal temperature from TGA/DSC but possessing significant differences in material purity and particle size. LNMO-LiCar showed the smallest material purity and largest particle size of 69.4% and 562 nm, respectively. Unfortunately, major impurities from the LiNiO contribute to the surface morphology and, as a result, deliver poor electrochemical performances, which can inhibit the release of lithium ions during battery operations. In contrast, LNMO-LiOH exhibits the highest specific capacity of up to 92.75 mAh/g, better cycle stability of around 40 cycles at C/5 current rates, as well as the lowest impurity and size. Despite LNMO-LiAce delivering a similar trend, the difference is insignificant for replacing LNMO-LiOH, even though it requires more complex production processes than the other two lithium sources. Therefore, the synthesis route used in this research is more suitable for LNMO-LiOH, and finally, it remains the preferred choice for lithium precursors. Further research is crucial for considering other synthesis routes for carbonate precursors in their potential for the sustainability of LNMO production, while the acetate precursors still need further optimization to deliver their synergistic effects with other acetate-based metal precursors.

Acknowledgments

This research was funded by grants from Lembaga Pengelola Dana Pendidikan (LPDP) through Riset dan Inovasi untuk Indonesia Maju (RIIM) and the National Research and Innovation Agency (BRIN) through Penelitian Rumah Program – Research Organization for Nanotechnology and Materials. The authors acknowledge the facilities, scientific, and technical support from E-Layanan Sains (ELSA) – Advanced Characterization Laboratories Serpong.

Author Contributions: S.: conceptualization, supervision, methodology, formal analysis, writing – review and editing; N.S.: data validation, writing – original draft; P.A.K.S.: data collection, data analysis, writing – original draft; A.C.F.: data analysis, writing – review and editing; A.A.S.: writing – original draft; E.B.N.: supervision, writing – review and editing; S.P.: CV analysis, writing – review and editing; H.J.: XRD analysis, writing – review and editing; M.D.G.: TGA/DSC analysis, writing – review. All authors have read and agreed to the published version of the manuscript.

Conflicts of Interest: The authors declare no conflict of interest.

References

Ahsan, Z., Ding, B., Cai, Z., Wen, C., Yang, W., Ma, Y., Zhang, S., Song, G., & Javed, M. S. (2021). Recent Progress in Capacity Enhancement of $LiFePO_4$ Cathode for Li-Ion Batteries. *Journal of Electrochemical Energy Conversion and Storage*, *18*(1). https://doi.org/10.1115/1.4047222

Cao, K., Shen, T., Wang, K., Chen, D., & Wang, W. (2017). Influence of different lithium sources on the morphology, structure and electrochemical performances of lithium-rich layered oxides. *Ceramics International*, *43*(12), 8694–8702. https://doi.org/10.1016/j.ceramint.2017.03.203

Chen, J., Huang, Z., Zeng, W., Cao, F., Ma, J., Tian, W., & Mu, S. (2021). Synthesis, Modification, and Lithium-Storage Properties of Spinel $LiNi_{0.5}Mn_{1.5}O_4$. *ChemElectroChem*, *8*(4), 608–624. https://doi.org/10.1002/celc.202001414

Chi, L. H., Dinh, N. N., Brutti, S., & Scrosati, B. (2010). Synthesis, characterization and electrochemical properties of 4.8V $LiNi_{0.5}Mn_{1.5}O_4$ cathode material in lithium-ion batteries. *Electrochimica Acta*, *55*(18), 5110–5116 . https://doi.org/10.1016/j.electacta.2010.04.003

Choi, J. U., Voronina, N., Sun, Y., & Myung, S. (2020). Recent Progress and Perspective of Advanced High-Energy Co-Less Ni-Rich Cathodes for Li-Ion Batteries: Yesterday, Today, and Tomorrow. *Advanced Energy Materials*, *10*(42). https://doi.org/10.1002/aenm.202002027

Fakhrudin, M., Sudaryanto, & Purwamargapratala, Y. (2021). Preparation and characterization of yttrium-doped high voltage spinel $LiNi_{0.5}Mn_{1.5}O_4$ for lithium-ion batteries. *AIP Conference Proceedings, 2381*, 020013. https://doi.org/10.1063/5.0066287

Feng, X. Y., Shen, C., Fang, X., & Chen, C. H. (2011). Synthesis of $LiNi_{0.5}Mn_{1.5}O_4$ by solid-state reaction with improved electrochemical performance. *Journal of Alloys and Compounds*,

509(8), 3623–3626. https://doi.org/10.1016/j.jallcom.2010.12.116

Ghosh, S., charjee, U. B., Bhowmik, S., & Martha, S. K. (2021). A Review on High-Capacity and High-Voltage Cathodes for Next-Generation Lithium-ion Batteries. *Journal of Energy and Power Technology*, *4*(1), 1–1. https://doi.org/10.21926/jept.2201002

Guo, K., Qi, S., Wang, H., Huang, J., Wu, M., Yang, Y., Li, X., Ren, Y., & Ma, J. (2022). High-Voltage Electrolyte Chemistry for Lithium Batteries. *Small Science*, *2*(5). https://doi.org/10.1002/smsc.202100107

Hu, Z. Q., Yang, D. X., Yin, K. J., Liu, J. X., Li, F., Gao, W. Y., Qin, Y., & Liu, H. (2013). The Effect of Lithium Source on the Electrochemical Performance of $LiFePO_4$/C Cathode Materials Synthesized by Sol-Gel Method. *Advanced Materials Research*, *669*, 311–315. https://doi.org/10.4028/www.scientific.net/AMR.669.311

Ihalainen, M., Kortelainen, M., Mesceriakovas, A., Karhunen, T., Mesceriakove, S.-M., Lindberg, D., Leskinen, J. T. T., Kankaanpää, T., Jokiniemi, J., & Lähde, A. (2023). Synthesis of solid NMC622 particles by spray drying, post-annealing and lithiation. *Advanced Powder Technology*, *34*(10), 104187. https://doi.org/10.1016/j.apt.2023.104187

Kelly, J. C., Dai, Q., & Wang, M. (2020). Globally regional life cycle analysis of automotive lithium-ion nickel manganese cobalt batteries. *Mitigation and Adaptation Strategies for Global Change*, *25*(3), 371–396. https://doi.org/10.1007/s11027-019-09869-2

Kong, F., Zhang, G., Wu, D., Sun, F., Tao, S., Chu, S., Qian, B., Chu, W., & Song, L. (2023). Insight into the cation migration and surface structural evolution of spinel $LiNi_{0.5}Mn_{1.5}O_4$ cathode material for lithium-ion batteries. *Chemical Engineering Journal*, *451*, 138708. https://doi.org/10.1016/j.cej.2022.138708

Kosova, N. V., Bobrikov, I. A., Podgornova, O. A., Balagurov, A. M., & Gutakovskii, A. K. (2016). Peculiarities of structure, morphology, and electrochemistry of the doped 5-V spinel cathode materials $LiNi_{0.5-x}Mn_{1.5-y}M_{x+y}O_4$ (M = Co, Cr, Ti; x+y = 0.05) prepared by mechanochemical way. *Journal of Solid State Electrochemistry*, *20*(1), 235–246. https://doi.org/10.1007/s10008-015-3015-4

Ku, D. J., Lee, J. H., Lee, S. J., Koo, M., & Lee, B. J. (2019). Effects of carbon coating on $LiNi_{0.5}Mn_{1.5}O_4$ cathode material for lithium ion batteries using an atmospheric microwave plasma torch. *Surface and Coatings Technology*, *376*, 25–30. https://doi.org/10.1016/j.surfcoat.2018.09.082

Lang, Y., Sun, X., Xue, G., Duan, X., Wang, L., & Liang, G. (2022). Synthesis and enhanced electrochemical performance of $LiNi_{0.5}Mn_{1.5}O_4$ cathode materials under the assistance of polyvinylpyrrolidone. *Ionics*, *28*(11), 5025–5038. https://doi.org/10.1007/s11581-022-04744-8

Li, J., Du, Z., Ruther, R. E., AN, S. J., David, L. A., Hays, K., Wood, M., Phillip, N. D., Sheng, Y., Mao, C., Kalnaus, S., Daniel, C., & Wood, D. L. (2017). Toward Low-Cost, High-Energy Density, and High-Power Density Lithium-Ion Batteries. *JOM*, *69*(9), 1484–1496. https://doi.org/10.1007/s11837-017-2404-9

Li, Y., Li, Z., Chen, C., Yang, K., Cao, B., Xu, S., Yang, N., Zhao, W., Chen, H., Zhang, M., & Pan, F. (2021). Recent progress in Li and Mn rich layered oxide cathodes for Li-ion batteries. *Journal of Energy Chemistry*, *61*, 368–385. https://doi.org/10.1016/j.jechem.2021.01.034

Lin, Y., Välikangas, J., Sliz, R., Molaiyan, P., Hu, T., & Lassi, U. (2023). Optimized Morphology and Tuning the Mn^{3+} Content of $LiNi_{0.5}Mn_{1.5}O_4$ Cathode Material for Li-Ion Batteries. *Materials*, *16*(8), 3116. https://doi.org/10.3390/ma16083116

Liu, Y.-H., Lin, H.-H., & Tai, Y.-J. (2018). Binder-free carbon fiber-based lithium-nickel-manganese-oxide composite cathode with improved electrochemical stability against high voltage: Effects of composition on electrode performance. *Journal of Alloys and Compounds*, *735*, 580–587. https://doi.org/10.1016/j.jallcom.2017.11.056

Luo, Y., Cui, Z., Wu, C., Sa, B., Wen, C., Li, H., Huang, J., Xu, C., & Xu, Z. (2023). Enhanced Electrochemical Performance of a Ti–Cr-Doped $LiMn_{1.5}Ni_{0.5}O_4$ Cathode Material for Lithium-Ion Batteries. *ACS Omega*, *8*(25), 22721–22731. https://doi.org/10.1021/acsomega.3c01524

Ma, C., Wang, L., Yang, H., & Liu, H. (2018). A Comparative Study of Synthesis Processes for $LiNi_{0.5}Mn_{1.5}O_4$ Cathode Material. *International Journal of Electrochemical Science*, *13*(8), 8170–8178. https://doi.org/10.20964/2018.08.53

Marceau, E., Che, M., Čejka, J., & Zukal, A. (2010). Nickel(II) Nitrate vs. Acetate: Influence of the Precursor on the Structure and Reducibility of Ni/MCM-41 and Ni/Al-MCM-41 Catalysts. *ChemCatChem*, *2*(4), 413–422. https://doi.org/10.1002/cctc.200900289

Mohamed, N., & Allam, N. K. (2020). Recent advances in the design of cathode materials for Li-ion batteries. *RSC Advances*, *10*(37), 21662–21685. https://doi.org/10.1039/D0RA03314F

Mohamedi, M., Makino, M., Dokko, K., Itoh, T., & Uchida, I. (2002). Electrochemical investigation of $LiNi_{0.5}Mn_{1.5}O_4$ thin film intercalation electrodes. *Electrochimica Acta*, *48*(1), 79–84. https://doi.org/10.1016/S0013-4686(02)00554-6

Mossali, E., Picone, N., Gentilini, L., Rodrìguez, O., Pérez, J. M., & Colledani, M. (2020). Lithium-ion batteries towards circular economy: A literature review of opportunities and issues of recycling treatments. *Journal of Environmental Management*, *264*, 110500. https://doi.org/10.1016/j.jenvman.2020.110500

Murdock, B. E., Toghill, K. E., & Tapia-Ruiz, N. (2021). A Perspective on the Sustainability of Cathode Materials used in Lithium-Ion Batteries. *Advanced Energy Materials*, *11*(39). https://doi.org/10.1002/aenm.202102028

Nguyen, V. T., Deferm, C., Caytan, W., Riaño, S., Jones, P. T., & Binnemans, K. (2023). Conversion of Lithium Chloride into Lithium Hydroxide by Solvent Extraction. *Journal of Sustainable Metallurgy*, *9*(1), 107–122. https://doi.org/10.1007/s40831-022-00629-2

Palaniyandy, N., Reddy, M. V., Zaghib, K., Kebede, M. A., Raju, K., Modibedi, R. M., Mathe, M. K., Abhilash, K. P., & Balamuralikrishnan, S. (2022). High rate and stable capacity performance of 2D $LiMn_{1.5}Ni_{0.5}O_4$ nanoplates cathode with ultra-long cycle stability. *Journal of Alloys and Compounds*, *903*, 163869. https://doi.org/10.1016/j.jallcom.2022.163869

Qin, X., Gong, J., Guo, J., Zong, B., Zhou, M., Wang, L., & Liang, G. (2019). Synthesis and performance of $LiNi_{0.5}Mn_{1.5}O_4$ cathode materials with different particle morphologies and sizes for lithium-ion battery. *Journal of Alloys and Compounds*, *786*, 240–249. https://doi.org/10.1016/j.jallcom.2019.01.307

Ronduda, H., Zybert, M., Szczęsna-Chrzan, A., Trzeciak, T., Ostrowski, A., Szymański, D., Wieczorek, W., Raróg-Pilecka, W., & Marcinek, M. (2020). On the Sensitivity of the Ni-rich Layered Cathode Materials for Li-ion Batteries to the Different Calcination Conditions. *Nanomaterials*, *10*(10), 2018. https://doi.org/10.3390/nano10102018

Shen, Y., Ju, X., Zhang, J., Xie, T., Zong, F., Xue, D., Lin, X., Zhang, J., & Li, Q. (2020). A convenient co-precipitation method to prepare high performance $LiNi_{0.5}Mn_{1.5}O_4$ cathode for lithium ion batteries. *Materials Chemistry and Physics*, *240*, 122137. https://doi.org/10.1016/j.matchemphys.2019.122137

Sivakumar, P., Nayak, P. K., Markovsky, B., Aurbach, D., & Gedanken, A. (2015). Sonochemical synthesis of $LiNi_{0.5}Mn_{1.5}O_4$ and its electrochemical performance as a cathode material for 5 V Li-ion batteries. *Ultrasonics Sonochemistry*, *26*, 332–339. https://doi.org/10.1016/j.ultsonch.2015.02.007

Sudaryanto, Fakhrudin, M., Purwamargapratala, Y., Yulianti, E., Deswita, & Wahyudianingsih. (2021). Synthesis of rare Earth element doped $LiMn_{1.5}Ni_{0.5}O_4$ as a lithium-ion battery cathode material using sonochemical method. *AIP Conference Proceedings, 2381*, 020084. https://doi.org/10.1063/5.0066454

Tian, Y., Zeng, G., Rutt, A., Shi, T., Kim, H., Wang, J., Koettgen, J., Sun, Y., Ouyang, B., Chen, T., Lun, Z., Rong, Z., Persson, K., & Ceder, G. (2021). Promises and Challenges of Next-Generation "Beyond Li-ion" Batteries for Electric Vehicles and Grid Decarbonization. *Chemical Reviews*, *121*(3), 1623–1669. https://doi.org/10.1021/acs.chemrev.0c00767

Ulu Okudur, F., Mylavarapu, S. K., Safari, M., De Sloovere, D., D'Haen, J., Joos, B., Kaliyappan, P., Kelchtermans, A.-S., Samyn, P., Van Bael, M. K., & Hardy, A. (2022). $LiNi_{0.5}Mn_{1.5}O_4$-δ (LNMO) as Co-free cathode for lithium ion batteries via solution-gel synthesis: Particle size and morphology investigation. *Journal of Alloys and Compounds*, *892*, 162175. https://doi.org/10.1016/j.jallcom.2021.162175

Wang, P.-B., Luo, M.-Z., Zheng, J.-C., He, Z.-J., Tong, H., & Yu, W. (2018). Comparative Investigation of $0.5Li_2MnO_3{\cdot}0.5LiNi_{0.5}Co_{0.2}Mn_{0.3}O_2$ Cathode Materials Synthesized by Using Different Lithium Sources. *Frontiers in Chemistry*, *6*, 159. https://doi.org/10.3389/fchem.2018.00159

Wang, Y., Hietaniemi, M., Välikangas, J., Hu, T., Tynjälä, P., & Lassi, U. (2023). Effects of Lithium Source and Content on the Properties of Li-Rich Layered Oxide Cathode Materials. *ChemEngineering*, *7*(1), 15. https://doi.org/10.3390/chemengineering7010015

Whittingham, M. S. (2004). Lithium Batteries and Cathode Materials. *Chemical Reviews*, *104*(10), 4271–4302. https://doi.org/10.1021/cr020731c

Wu, C., Qiu, L., Wang, D., Chen, T., Li, J., Wu, Z., Song, Y., & Guo, X. (2022). New Insight into High-Rate Performance Lithium-Rich Cathode Synthesis through Controlling the Reaction Pathways by Low-Temperature Intermediates. *Industrial & Engineering Chemistry Research*, *61*(1), 453–463. https://doi.org/10.1021/acs.iecr.1c04464

Wu, T., Ma, X., Liu, X., Zeng, G., & Xiao, W. (2015). Effect of calcination temperature on electrochemical performances of $LiFePO_4$/C cathode material. *Materials Technology*, *30*(sup2), A70–A74. https://doi.org/10.1179/17535557A15Y.000000011

Wu, W., Zuo, S., Zhang, X., & Feng, X. (2023). Two-Step Solid State Synthesis of Medium Entropy $LiNi_{0.5}Mn_{1.5}O_4$ Cathode with Enhanced Electrochemical Performance. *Batteries*, *9*(2), 91. https://doi.org/10.3390/batteries9020091

Xu, X., Deng, S., Wang, H., Liu, J., & Yan, H. (2017). Research Progress in Improving the Cycling Stability of High-Voltage $LiNi_{0.5}Mn_{1.5}O_4$ Cathode in Lithium-Ion Battery. *Nano-Micro Letters*, *9*(2), 22. https://doi.org/10.1007/s40820-016-0123-3

Yi, T.-F., Li, C.-Y., Zhu, Y.-R., Shu, J., & Zhu, R.-S. (2009). Comparison of structure and electrochemical properties for 5 V $LiNi_{0.5}Mn_{1.5}O_4$ and $LiNi_{0.4}Cr_{0.2}Mn_{1.4}O_4$ cathode materials. *Journal of Solid State Electrochemistry*, *13*(6), 913–919. https://doi.org/10.1007/s10008-008-0628-x

Yi, T.-F., Li, Y.-M., Li, X.-Y., Pan, J.-J., Zhang, Q., & Zhu, Y.-R. (2017). Enhanced electrochemical property of $FePO_4$-coated $LiNi_{0.5}Mn_{1.5}O_4$ as cathode materials for Li-ion battery. *Science Bulletin*, *62*(14), 1004–1010. https://doi.org/10.1016/j.scib.2017.07.003

Yi, T.-F., Mei, J., & Zhu, Y.-R. (2016). Key strategies for enhancing the cycling stability and rate capacity of $LiNi_{0.5}Mn_{1.5}O_4$ as high-voltage cathode materials for high power lithium-ion batteries. *Journal of Power Sources*, *316*, 85–105. https://doi.org/10.1016/j.jpowsour.2016.03.070

Zeng, F., Zhang, Y., Shao, Z., Li, Z., & Dai, S. (2021). The influence of different calcination temperatures and times on the chemical performance of $LiNi_{0.5}Mn_{1.5}O_4$ cathode materials. *Ionics*, *27*(9), 3739–3748. https://doi.org/10.1007/s11581-021-04167-x

Zhang, B., Ou, X., Zheng, J., shen, C., Ming, L., Han, Y., Wang, J., & Qin, S. (2014). Electrochemical properties of $Li_2FeP_2O_7$ cathode material synthesized by using different lithium sources. *Electrochimica Acta*, *133*, 1–7. https://doi.org/10.1016/j.electacta.2014.03.188

Zybert, M., Ronduda, H., Szczęsna, A., Trzeciak, T., Ostrowski, A., Żero, E., Wieczorek, W., Raróg-Pilecka, W., & Marcinek, M. (2020). Different strategies of introduction of lithium ions into nickel-manganese-cobalt carbonate resulting in $LiNi_{0.6}Mn_{0.2}Co_{0.2}O_2$ (NMC622) cathode material for Li-ion batteries. *Solid State Ionics*, *348*, 115273. https://doi.org/10.1016/j.ssi.2020.115273